2024 IEEE 20th International Conference on Automation
Science and Engineering (CASE)
August 28 - September 1, 2024. Bari, Italy

2024 IEEE 20th International Conference on Automation Science and Engineering (CASE) | 979-8-3503-5851-3/24/$31.00 ©2024 IEEE | DOI: 10.1109/CASE59546.2024.10711536

FIT3D: Real-time Flatness Inspection Algorithm for Ceramic Tiles using the Structured Light 3D Scanner*

Yukun Xie, Juan Du, *Member, IEEE*, Fugee Tsung, *Member, IEEE*, Peng Wan and Guanghua Xu

***Abstract*— The accurate inspection of surface flatness is important for the quality inspection of ceramic tiles. According to quality standards, the flatness value is evaluated based on the surface information of ceramic tiles. Current industry practice relies on manual inspection or displacement sensors to collect surface information, which has limitations in accuracy due to incomplete surface information. Structured light 3D scanners can offer more comprehensive surface information and more accurate flatness inspection. However, processing large-scale point cloud data from the 3D scanner in real time presents a significant challenge. To address this challenge, we propose a real-time flatness inspection algorithm for ceramic tiles using the structured light 3D scanner (FIT3D). FIT3D utilizes a support vector machine (SVM) model to deal with the large-scale point cloud and determine the minimum zone planes. The convex hull theory is then combined within the model to speed up the algorithm. The effectiveness of the algorithm is demonstrated through studies on several datasets in literature and a real-world case study.**

I. Introduction

The ceramic tile industry is crucial in both the construction sector and economic growth. As reported in previous studies [1], it has been found that, on average, 11% of ceramic products fail to meet the required quality standards. Among the quality issues, almost 73% are due to planarity defects [2], which means that the surface flatness of ceramic tiles is out of the control limits. Thus, the accurate evaluation of surface flatness is vital for the quality inspection of ceramic tiles.

There have been standards [3, 4] that define the instruments and the specific steps to conduct flatness inspection. However, different manufacturers have their own inspection methods and definitions of flatness in practice. A more general definition of flatness can be found in ISO 12781-1-2011 [5], ASME Y14.5-2018 [6], and GB/T 11337-2004 [7], which is the deviation from the point on the surface to an ideal reference plane. Recommended by ISO [5], the reference plane is determined by the minimum zone method (MZM) based on the axis of sampling points on the surface. As shown in Figure 1, MZM tries to find two parallel planes called minimum zone planes. The two parallel planes are expected to enclose all the sampling points, and the smallest distance between the two minimum zone planes is the inspected flatness value. According to MZM, the manufacturers can evaluate the surface flatness of ceramic tiles based on surface information.

Currently, practitioners in the ceramic industry mostly rely on manual inspection for collecting surface information and flatness inspection. As shown in Figure 2 (a), a steel ruler is used as a reference, and a feeler gauge is used to measure the gap width between the ruler and the ceramic surface. The feeler gauge in Figure 2 (b) consists of steel blades of different thicknesses. The maximum gap width is used to determine the flatness along the direction of the ruler, with results recorded as shown in Figure 2 (c). The limitation is that the manual inspection method only applies to sampling quality inspection, while the high-end ceramic tile products urge precise flatness inspection for each tile. Additionally, as shown in Figure 2 (a), the result of the manual inspection method is only the deviation to a reference line, not a reference surface. Therefore, the information used by manual inspection is incomplete, and the loss of information from the whole surface can lead to biased results and underestimation of surface flatness.

There have also been practices using displacement sensors instead of manual inspection. However, the information from displacement sensors is still incomplete. For example, the displacement sensors are placed to collect the profile of the scanned surface [8, 9]. The collected profile shows the displacement in a specific direction, and the flatness can be obtained from the profile. The complete surface can be scanned with a set of displacement sensors, while the information is incomplete due to the limit of sensor number.

Therefore, a flatness inspection method based on the information of the whole surface is desired for accurate dimensional quality evaluation. The 3D scanners can generate large amounts of data from surface measurements of the product surface. This data is often referred to as 3D point cloud

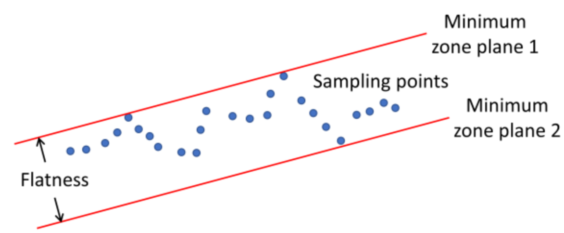

Fig. 1. Definition of minimum zone planes.

*Research supported in part by the National Natural Science Foundation of China (No. 72001139, No. 72371219, and No. 52372308), Guangdong Basic and Applied Basic Research Foundation (No. 2023A1515011656), and Guangzhou-HKUST(GZ) Joint Funding Program under Grant No. 2023A03J0651. (Corresponding author: Juan Du).

Yukun Xie is with the Smart Manufacturing Thrust, Systems Hub, The Hong Kong University of Science and Technology (Guangzhou), Guangzhou 511400, China (e-mail: yukun.xie@connect.ust.hk).

Juan Du is with the Smart Manufacturing Thrust, Systems Hub, The Hong Kong University of Science and Technology (Guangzhou), Guangzhou 511400, China. Juan Du is also with the Department of Mechanical and Aerospace Engineering, The Hong Kong University of Science and Technology, Hong Kong SAR, China and Guangzhou HKUST Fok Ying Tung Research Institute, Guangzhou 511458, China. (Corresponding author to provide phone: (86)020-88335989; e-mail: juandu@ust.hk).

Fugee Tsung is with The Hong Kong University of Science and Technology and The Hong Kong University of Science and Technology (Guangzhou), Guangzhou, China (Email: season@ust.hk).

Peng Wan and Guanghua Xu are with Jumper Thermal Energy Technology, Foshan 528000, China (e-mail: 13802620665@139.com; 13790010295@163.com)

Fig. 2. (a) Illustration of manual inspection; (b) Feeler gauge used to measure the gap width; (c) Recordings of manual inspection results.

data, which provides the entire external surface geometry of the scanned surface. Recently, the mature technique and lower cost of 3D scanners have made it possible to apply to ceramic tile production and achieve more accurate and efficient flatness inspection than manual inspection and displacement sensors.

However, a flatness inspection algorithm is needed for the point cloud data from the 3D scanner, and the development of the algorithm poses the following challenges:

- Large-scale Point Cloud. The point cloud for a single ceramic tile contains more than one million points due to the large size of high-end ceramic tile products. The determination of the minimum zone planes is a non-convex optimization problem. Therefore, it is challenging for the algorithm to acquire the minimum zone planes which can enclose numerous points and have the smallest distance.
- Real-time Inspection. The inspection method is expected to inspect each ceramic tile on the production line in real time and achieve total quality inspection. The high computational cost of the algorithm will hinder the algorithm from application.

The algorithms to determine the minimum zone planes given point cloud data have been studied over the past years. The solution of the minimum zone planes can be based on computational geometry algorithms [10, 11], which use the convex hull theory and search for the best solution in a brute-force way. There have also been methods based on evolutionary algorithms [12] or approximation [13], but they cannot guarantee the global optimum. The common limitation of these algorithms is that the algorithms are initially designed for the point cloud data collected with a coordinate measuring machine (CMM). Compared to the point cloud of less than 100 points from CMM, the point cloud of more than millions of points from 3D scanners means that current algorithms cannot be directly applied to the input from 3D scanners. Although pioneering efforts [14-16] have endeavored to study the application of 3D scanners to evaluate ceramic tile surface quality, the focus is only on the design and implementation of the metrology system, not the flatness inspection algorithm.

To tackle the challenges of dealing with large-scale point cloud and real-time inspection, we propose the FIT3D algorithm. The algorithm applies an SVM model to find minimum zone planes from millions of points acquired from large-sized ceramic tiles. The convex hull theory further speeds up the solution of the SVM model.

The main contributions of our algorithm are as follows:

- To the best of our knowledge, we are the first effort to study the flatness inspection algorithm of ceramic tiles with 3D scanners.
- We identify the benefits of applying the SVM model to deal with the large-scale point cloud. The SVM model transforms the problem of determining minimum zone planes into the problem of optimizing the parameters of supporting planes, which can be efficiently solved with a gradient descent algorithm.
- Through the combination of convex hull theory, we eliminate redundant points for the solution of the SVM model and the evaluation of flatness, which can significantly reduce the computation cost and make real-time inspection possible.

The subsequent sections of the paper are structured as follows. Section II reviews the algorithms for the determination of minimum zone planes. The FIT3D algorithm is elaborated in Section III, including the SVM model and its combination with convex hull theory. In Section IV, our method is compared with benchmarks on several datasets from CMM and one point cloud from the 3D scanner to validate its effectiveness. Finally, Section V concludes the paper.

II. Related Works

We review the current literature from two perspectives. The first subsection reviews algorithms to determine minimum zone planes. The second subsection introduces the previous applications of 3D scanners for ceramic tile surface flatness inspection.

A. Literature for Algorithms to Determine Minimum Zone Planes

Traditional algorithms to determine minimum zone planes can be divided into three categories: convex hull-based methods, evolutionary algorithms-based methods, and approximation-based methods.

Starting from [10], the convex hull theory has been employed to help determine the minimum zone planes. The convex hull is defined as the boundary of the minimum convex domain containing all the data points. In [10], all the vertex points on the convex hull were identified, and then all the combinations of convex hull faces and farthest points were searched in a brute-force way. The smallest value of the distance between convex hull faces and farthest points is the flatness value. Similarly, all the combinations of convex hull faces and farthest points and combinations of convex hull edges and farthest edges were enumerated in [17]. In contrast,

[18] converted the problem of finding the farthest point to each convex hull face in 3D coordinate space into finding the farthest point to each convex hull edge in 2D coordinate space. By projecting the points onto a 2D plane, the computational cost can be reduced. [18] constructed the 2D convex hull for the projected points on the 2D plane to find the farthest point. [11] proposed a more efficient method than [18] without constructing 2D convex hulls. [19] further improved the efficiency of the algorithm by narrowing down the search area of convex hull edges, rather than enumerating all the convex hull edges. Although the convex hull-based methods can guarantee the global optimum and find the minimum flatness value, enumerating the large-scale point cloud from 3D scanner can be time-consuming.

Evolutionary algorithms have been applied to optimize minimum zone plane parameters, such as the genetic algorithm [20] and particle swarm algorithm [12, 21]. Nevertheless, the accuracy of evolutionary algorithms is highly dependent on the settings of hyperparameters and updating strategies, which may not be suitable for real-time inspection applications.

The approximation-based methods first approximate the non-convex problem of determining minimum zone planes with mathematical models, and then use the solutions of mathematical models to determine minimum zone planes. Some typical models for approximation include the linear programming model [22, 23] and the simplex search model [13]. For example, [22, 23] approximated the problem of determining minimum zone planes with linear programming problems. However, the linearization will significantly reduce the accuracy of flatness inspection results. [13] transformed the problem of determining minimum zone planes into the search for a 2D simplex. Nevertheless, the update of the simplex is in a fixed mode and cannot obtain the solution efficiently.

The SVM is another promising model for approximating the problem of determining minimum zone planes. By transforming the non-convex problem into the problem of optimizing the parameters of SVM hyperplanes, the SVM has been successfully applied to evaluate surface flatness in previous studies [24-26]. Unlike other mathematical models, the SVM model is interpretable and can be efficiently solved with a gradient descent algorithm [24]. Moreover, the approximation based on SVM can handle the large-scale point cloud from the 3D scanner, although the number of constraints of the SVM grows linearly with the number of points. Therefore, further improvements in the computational efficiency of the SVM model for the large-scale point cloud can be explored.

B. *Literature for Surface Flatness Inspection of Ceramic Tile based on 3D Scanners*

Currently, the 3D metrology used for surface flatness inspection of ceramic tile includes the laser line 3D scanner and phase measurement. [14] devised a metrology system based on a laser line 3D scanner for the quality inspection of small-sized extreme wall tiles. The flatness is defined as the maximum deviation to the reference plane, but the determination of the reference plane is not discussed in [14]. Similarly, [15] applied the laser line 3D scanner to detect flatness defects while the reference plane of the ceramic surface is assumed to be known in advance. Using phase measurement, [16] implemented a metrology system to acquire the point cloud of the ceramic surface. The convex hull theory is applied to help deal with the large-scale point cloud. However, the reference plane is determined by the least square method (LS), which brings bias and is not recommended by the quality standard [5].

III. Methodology

In this section, we introduce the model and procedures of our FIT3D framework. The large-scale point cloud from large-sized ceramic tiles and the real-time inspection requirement mean that the algorithm should obtain the minimum zone planes accurately and efficiently. As shown in Figure 3, our FIT3D first computes the convex hull of the input point cloud, and the convex hull vertices are then used to determine the minimum zone planes 1 and 2. We apply the modified SVM model in [24] to obtain the parameters of minimum zone planes. The optimization problem for SVM can be solved in seconds since we only need to compute on a small subset of the point cloud using the convex hull theory. Finally, the surface flatness is estimated with the distance between minimum zone planes 1 and 2.

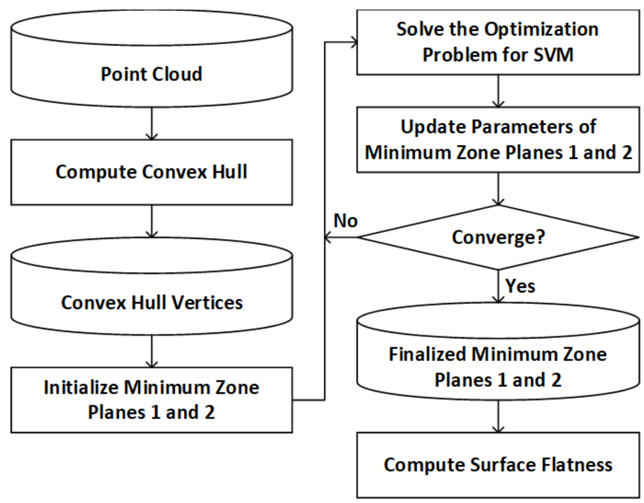

Fig. 3. Flowchart of the FIT3D framework.

Section III-A briefly introduces the formulation of our problem and the modified SVM model. Section III-B illustrates the detailed procedures of the framework. Section III-C analyzes the computational complexities of our method and benchmarks.

A. *Problem Formulation*

The evaluation of the surface flatness is based on the minimum zone planes. Suppose that the point cloud acquired from a ceramic tile contains N points, we denote the 3D axis of N data points as $\boldsymbol{x}_i, i = 1, \dots, N$. The minimum zone planes 1 and 2 are denoted as two parallel planes H_1 and H_2 in 3D coordinate space:

$$H_1: Ax + By + Cz + D - 1 = 0, \quad (1)$$

$$H_2: Ax + By + Cz + D + 1 = 0, \quad (2)$$

where A, B, C, and D are parameters of the two parallel planes H_1 and H_2. The goal of determining minimum zone planes is to let H_1 and H_2 enclose all the N data points and have the smallest distance to each other.

SVM aims to construct hyperplanes in high dimensions for further classification or regression tasks. The hyperplanes are expected to have the largest distance to the training data of any class so that the hyperplanes can separate the data of each class. Contrary to the traditional SVM, the two hyperplanes in the modified SVM are expected to have the smallest distance [24]. Therefore, the goal of the modified SVM is consistent with the goal of determining minimum zone planes. Once the hyperplanes with the smallest distance are found, we consider the two hyperplanes as the minimum zone planes H_1 and H_2. The problem of the modified SVM in [24] can then be formulated as follows:

$$max\frac{1}{2}(A^2+B^2+C^2) \tag{3}$$

$$s.t.\ \boldsymbol{x}_i{}^T\begin{bmatrix}A\\B\\C\end{bmatrix}+D\le 1, i=1,\dots,N$$

$$-\boldsymbol{x}_i{}^T\begin{bmatrix}A\\B\\C\end{bmatrix}-D\le 1, i=1,\dots,N \tag{4}$$

The optimization problem in Equations (3-4) is non-convex. To obtain the solution to the optimization problem, [24] has proposed a gradient descent procedure, as shown in Equation (5-7). We use A_k, B_k, C_k, and D_k to denote the minimum zone plane parameters at iteration k. In each iteration, the sub-problem in Equations (5-6) is solved to obtain the optimal values of gradients A_0, B_0, C_0, and D_0. A_k, B_k, C_k, and D_k are then updated with Equation (7).

$$\max\begin{bmatrix}A_k\\B_k\\C_k\end{bmatrix}^T\cdot\begin{bmatrix}\Delta A\\\Delta B\\\Delta C\end{bmatrix} \tag{5}$$

$$s.t.\ \boldsymbol{x}_i{}^T\begin{bmatrix}A_k\\B_k\\C_k\end{bmatrix}+\boldsymbol{x}_i{}^T\begin{bmatrix}\Delta A\\\Delta B\\\Delta C\end{bmatrix}+D_k+\Delta D\le 1, i=1,\dots,N$$

$$-\boldsymbol{x}_i{}^T\begin{bmatrix}A_k\\B_k\\C_k\end{bmatrix}-\boldsymbol{x}_i{}^T\begin{bmatrix}\Delta A\\\Delta B\\\Delta C\end{bmatrix}-D_k-\Delta D\le 1, i=1,\dots,N \tag{6}$$

$$A_{k+1}=A_k+\Delta A, B_{k+1}=B_k+\Delta B,$$
$$C_{k+1}=C_k+\Delta C, D_{k+1}=D_k+\Delta D. \tag{7}$$

The sub-problem in Equations (5-6) is a linear programming problem and can be easily solved. The only problem is that, as shown in Equation (6), we will have millions of constraints when dealing with a large-scale point cloud. The optimization problem may not be solved efficiently given millions of constraints, so the modified SVM cannot be directly applied to our case.

B. Procedures of the Framework

This subsection presents the detailed procedures to evaluate surface flatness based on the convex hull theory and the modified SVM model.

Firstly, we compute the convex hull of the raw point cloud with the QuickHull algorithm [27]. We denote the convex hull vertices as $\boldsymbol{x'}_i, j=1,\dots,N_h$, where N_h denotes the number of vertices on the convex hull. According to the definitions of the convex hull, the points on the hyperplanes of SVM should be the convex hull vertices. Therefore, we only focus on the vertices of the convex hull when solving the SVM or estimating the flatness value.

Afterwards, we apply the modified SVM model in Section III-A. To solve the minimum zone planes with parameters A, B, C, and D, we first initialize the minimum zone plane with LS or random sample consensus (RANSAC). The initial solution A_0, B_0, C_0, and D_0 are then used in the subproblem in Equations (5-6). We iteratively update A_k, B_k, C_k, and D_k with Equation (7) until $\delta<\delta'$. δ' is the pre-specified threshold to stop the gradient descent procedure, and δ defined in Equation (8) is the difference between two adjacent flatness estimations with A_{k+1}, B_{k+1}, C_{k+1}, D_{k+1} and A_k, B_k, C_k, D_k.

$$\delta=\left|\frac{\frac{2}{\sqrt{{A_{k+1}}^2+{B_{k+1}}^2+{C_{k+1}}^2}}-\frac{2}{\sqrt{{A_k}^2+{B_k}^2+{C_k}^2}}}{\frac{2}{\sqrt{{A_k}^2+{B_k}^2+{C_k}^2}}}\right|. \tag{8}$$

The finalized minimum zone planes H_1 and H_2 are then determined with parameters A_k, B_k, C_k, and D_k.

Finally, we estimate the flatness value d with $2/\sqrt{{A_k}^2+{B_k}^2+{C_k}^2}$, which is the distance between H_1 and H_2.

The proposed FIT3D algorithm is shown in Algorithm 1. The optimization problem formulated by Equation (5) and (6) is solved by us with the interior-point method with precision ε. Therefore, our FIT3D framework only has two hyperparameters ε and δ', which control the precision of the final solution and each sub-problem.

Algorithm 1: FIT3D

Input: Raw point cloud $\boldsymbol{x}_i, i=1,\dots,N$; Threshold to stop gradient descent procedure δ'; Precision of interior-point method ε;

Output: Surface flatness d;

Compute convex hull using QuickHull

Obtain convex hull vertices $\boldsymbol{x'}_i, j=1,\dots,N_h$

For $k=0$:

- Initialize A_0, B_0, C_0, and D_0 using LS or RANSAC

For $k>0$:

- Solve the optimization problem in Equations (5-6) using interior-point method with precision ε
- Obtain the gradients ΔA, ΔB, ΔC, and ΔD
- Update the parameters $A_{k+1}=A_k+\Delta A$, $B_{k+1}=B_k+\Delta B$, $C_{k+1}=C_k+\Delta C$, $D_{k+1}=D_k+\Delta D$
- Compute the difference δ with Equation (8)
- Stop if $\delta<\delta'$

Obtain finalized minimum zone planes H_1 and H_2 with parameters A_k, B_k, C_k, and D_k

Compute the surface flatness $d=\frac{2}{\sqrt{{A_k}^2+{B_k}^2+{C_k}^2}}$

TABLE I

COMPARISON OF TIME COMPLEXITY FOR BENCHMARKS AND FIT3D

Method	Time Complexity
M. T. Traband et al. 1989 [10]	$O(N^2)$
M.-K. Lee 1997 [18]	$O(N^2 logN)$
G. Hermann 2007 [17]	$O(N^2 + {N_e}^2)$
M.-K. Lee 2009 [11]	$O(NlogN + {N_h}^2)$
P. Li et al. 2016 [19]	$O(NlogN + N_c N_e + N_c N_h)$
M. Zhang et al. 2020 [12]	$O(NlogN + msN_h)$
FIT3D	$O\left(NlogN + mn^{3.5} log\frac{1}{\varepsilon}\right)$

C. Computational Complexity

To illustrate the efficiency of our FIT3D, we analyze the computational complexity of FIT3D and compare with the benchmark methods. Notably, we only analyze the time complexity since we care whether our method is suitable for real-time inspection.

Our algorithm has two main steps: the first step is the computation of convex hull, which is achieved through the QuickHull algorithm [27] with time complexity $O(NlogN)$; the second step is the solution of the modified SVM. Suppose m iterations are performed before the stopping criterion $\delta < \delta'$. In each iteration, the optimization problem is solved through the interior-point method with time complexity $O\left(n^{3.5} log\frac{1}{\varepsilon}\right)$, where n denotes the number of variables in the optimization problem. Therefore, the overall time complexity of the proposed FIT3D is $O\left(NlogN + mn^{3.5} log\frac{1}{\varepsilon}\right)$.

The time complexities of benchmark methods involving the application of convex hull theory are reviewed, including the convex hull-based methods [10, 11, 17-19] and one evolutionary algorithms-based method [12]. Table I summarizes the time complexities of the selected methods and our FIT3D. In Table I, N_e denotes the number of edges on the convex hull and N_c is the number of edges satisfying the searching area in [19]. s is the number of iterations for the particle swarm algorithm in [12].

Notably, N_h is still large when we are dealing with the point cloud from large-sized and complex surfaces. Taking our case as an example, large-sized ceramic tiles may have hundreds of vertices, which is a large value to enumerate all the situations. In worst cases, $N_h \approx N$ and the computational cost is not reduced for convex hull-based methods. In the part of our method that follows the convex hull computation, the time complexity is independent of N_h. Therefore, our FIT3D is expected to outperform the convex hull-based methods in computation speed given a large N_h value.

IV. EVALUATION

In this section, we apply the proposed FIT3D framework to the real data collected with 3D scanners from large-sized ceramic tiles. To validate the accuracy of our method and implemented benchmarks, we also experiment on three real datasets from CMM. The results of our FIT3D are compared with the flatness value reported in the literature and the results of implemented benchmark methods.

TABLE II

COMPARISON OF PERFORMANCE ON THE POINT CLOUD FROM CMM

Dataset	N	N_h	Method	Time (s)	Flatness (mm)
K. Carr and P. Ferreira 1995	25	13	M.-K. Lee 2009	0.0133	0.00486364
			P. Li et al. 2016	0.3222	0.00486364
			FIT3D	0.0177	0.00486364
T. Weber et al. 2002	20	13	M.-K. Lee 2009	0.0124	0.00261288
			P. Li et al. 2016	0.2826	0.00261288
			FIT3D	0.0173	0.00261289
G. Deng et al. 2003	25	14	M.-K. Lee 2009	0.0149	0.00713600
			P. Li et al. 2016	0.6009	0.00713600
			FIT3D	0.0176	0.00713600

TABLE III

COMPARISON OF PERFORMANCE ON THE POINT CLOUD FROM 3D SCANNER

Dataset	N	N_h	Method	Time (s)	Flatness (mm)
Ceramic tile of size 600mm*1200mm	2904569	392	M.-K. Lee 2009	6.4973	0.965891
			P. Li et al. 2016	18.0436	0.965891
			FIT3D	0.5971	0.965731

Several convex hull-based methods, including [11] and [19], are selected as the benchmark methods. We have implemented [11] and [19] following the algorithm flow in the literature. For the computation of the convex hull, we applied the QuickHull algorithm [27], which guarantees the time complexity in $O(NlogN)$. Both our algorithm and benchmarks are implemented with Python 3.8 and the optimization problems are solved with the package CVXPY.

We employ the RANSAC to obtain the initial solution A_0, B_0, C_0, and D_0 of the minimum zone planes. The RANSAC is performed on a point cloud uniformly sampled from the raw point cloud. The hyperparameters are set as $\varepsilon = 1 \times 10^{-8}$ and $\delta' = 0.01$ in our FIT3D framework.

The datasets from CMM in [22, 23, 28] are selected to validate the accuracy of our implementations. The descriptions of the datasets and results are given in Table II. As shown in Table II, our FIT3D obtains the same flatness value as the implemented benchmarks. The results are consistent with the flatness value reported in [19, 22, 28]. Therefore, our implementations of the benchmark methods are correct, and our FIT3D can realize the accurate inspection of flatness.

To validate the accuracy and efficiency of our method in real applications, we compare the results of our FIT3D with benchmark methods on the real data from the 3D scanner. The point cloud is collected from a ceramic tile of size 600mm*1200mm, and the visualizations of the point cloud and convex hull are shown in Figure 4. The red lines represent the convex hull edges, and the blue dots represent the vertices of the convex hull in Figure 4 (b). We can find that the number of points is significantly reduced after the convex hull computation. As illustrated in Table III, compared to the point cloud from CMM, the large-scale point cloud from the 3D scanner has a much larger number of points N and a larger number of convex hull vertices N_h. The large N_h means that the enumeration of convex hull-based methods will take much longer time. We can find that the computation time of our FIT3D is only around 9.2% of [11] and 3.3% of [19] with comparable accuracy. Notably, the computation time of our method is only 0.6 seconds for a ceramic tile, which means that the real-time flatness inspection on the conveyors of production line can be facilitated.

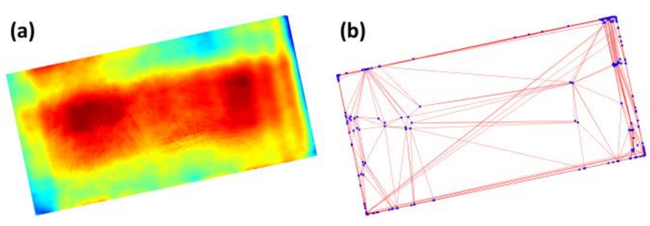

Fig. 4. (a) Visualization of the point cloud from large-sized ceramic tiles; (b) Visualization of the convex hull.

V. Conclusion

This paper proposed a real-time flatness inspection algorithm for ceramic tiles using the structured light 3D scanner. Compared to the current flatness inspection method based on manual inspection and displacement sensors, using 3D scanners presents an opportunity for a more comprehensive and accurate flatness inspection method. However, the development of a real-time algorithm for processing the large-scale point cloud is challenging. To tackle the challenges, we applied the SVM model to deal with the large-scale point cloud, which can obtain minimum zone planes for further flatness inspection. Moreover, the convex hull theory is used to eliminate redundant points, which reduces the computation time and enables real-time inspection.

The effectiveness of the FIT3D algorithm is validated through comparisons with benchmarks on several datasets from CMM and point cloud data from the 3D scanner. Compared with the benchmarks, the proposed FIT3D algorithm can obtain an accurate flatness value with less computation time on the point cloud data. Thus, the FIT3D algorithm has the potential to significantly improve the accuracy and efficiency of flatness inspection in the ceramic tile industry.

Although our FIT3D is proposed for ceramic tile surface flatness inspection, the methodology is also applicable to the flatness inspection of large-sized objects, such as steel strip and flange. However, the accuracy of FIT3D is influenced by the point cloud accuracy in real industry. If the scanned object is too large or there are disturbances in the scanning environment, the acquired point cloud will have large noise. The future work will be the improvement of our SVM model to make FIT3D robust to the noisy point cloud.

References

[1] T. Bonavia and J. A. Marin, "An Empirical Study of Lean Production in the Ceramic Tile Industry in Spain," *International Journal of Operations & Production Management,* vol. 26, no. 5, pp. 505-531, 2006.

[2] A. Al-Refaie and A. Diabat, "Optimizing Convexity Defect in a Tile Industry Using Fuzzy Goal Programming," *Measurement,* vol. 46, no. 8, pp. 2807-2815, 2013.

[3] *Test Methods of Ceramic Tiles - Part 2: Determination of Dimensions and Surface Quality, GB/T 3810.2-2016*, Beijing, China, 2016.

[4] *Ceramic Tiles - Part 2: Determination of Dimensions and Surface Quality, ISO 10545-2-2018*, 2018.

[5] *Geometrical Product Specifications (Gps) - Flatness - Part 1: Vocabulary and Parameters of Flatness, ISO 12781-1-2011*, 2011.

[6] *Dimensioning and Tolerancing, ASME Y14.5-2018*, New York, USA, 2018.

[7] *Measurement of Departures from Flatness, GB/T 11337-2004*, Beijing, China, 2004.

[8] G. Bakos, N. Tsagas, J. Lygouras, and J. Lucas, "Long Distance Non-Contact High Precision Measurements," *International Journal of Electronics Theoretical and Experimental,* vol. 75, no. 6, pp. 1269-1279, 1993.

[9] S. H. Hajimowlana, R. Muscedere, G. A. Jullien, and J. W. Roberts, "Defect Detection in Web Inspection Using Fuzzy Fusion of Texture Features," in *2000 IEEE International Symposium on Circuits and Systems (ISCAS)*, 2000, vol. 3: IEEE, pp. 718-721.

[10] M. T. Traband, S. Joshi, R. A. Wysk, and T. M. Cavalier, "Evaluation of Straightness and Flatness Tolerances Using the Minimum Zone," *Manufacturing Review,* vol. 2, no. 3, pp. 189-195, 1989.

[11] M.-K. Lee, "An Enhanced Convex-Hull Edge Method for Flatness Tolerance Evaluation," *Computer-Aided Design,* vol. 41, no. 12, pp. 930-941, 2009.

[12] M. Zhang, Y. Liu, C. Sun, X. Wang, and J. Tan, "Precision Measurement and Evaluation of Flatness Error for the Aero-Engine Rotor Connection Surface Based on Convex Hull Theory and an Improved Pso Algorithm," *Measurement Science and Technology,* vol. 31, no. 8, p. 085006, 2020.

[13] S. Damodarasamy and S. Anand, "Evaluation of Minimum Zone for Flatness by Normal Plane Method and Simplex Search," *IIE Transactions,* vol. 31, no. 7, pp. 617-626, 1999.

[14] J. Wu, "Research on Key Technology of Tile Quality Inspection System Based on Vision," MA Thesis, Huazhong University of Science and Technology, 2017.

[15] A. Sioma, "Automated Control of Surface Defects on Ceramic Tiles Using 3d Image Analysis," *Materials,* vol. 13, no. 5, p. 1250, 2020.

[16] Z. Ren, "Research on Ceramic Tile Flatness Detection Technology Based on Phase Measurement," MA Thesis, Xi'an University of Science and Technology, 2018.

[17] G. Hermann, "Robust Convex Hull-Based Algorithm for Straightness and Flatness Determination in Coordinate Measuring," *Acta Polytechnica Hungarica,* vol. 4, no. 4, pp. 111-120, 2007.

[18] M.-K. Lee, "A New Convex-Hull Based Approach to Evaluating Flatness Tolerance," *Computer-Aided Design,* vol. 29, no. 12, pp. 861-868, 1997.

[19] P. Li, X.-M. Ding, J.-B. Tan, and J.-W. Cui, "A Hybrid Method Based on Reduced Constraint Region and Convex-Hull Edge for Flatness Error Evaluation," *Precision Engineering,* vol. 45, pp. 168-175, 2016.

[20] R. Sharma, K. Rajagopal, and S. Anand, "A Genetic Algorithm Based Approach for Robust Evaluation of Form Tolerances," *Journal of Manufacturing Systems,* vol. 19, no. 1, pp. 46-57, 2000.

[21] Y. Kovvur, H. Ramaswami, R. B. Anand, and S. Anand, "Minimum-Zone Form Tolerance Evaluation Using Particle Swarm Optimisation," *International Journal of Intelligent Systems Technologies and Applications,* vol. 4, no. 1-2, pp. 79-96, 2008.

[22] K. Carr and P. Ferreira, "Verification of Form Tolerances Part I: Basic Issues, Flatness, and Straightness," *Precision Engineering,* vol. 17, no. 2, pp. 131-143, 1995.

[23] T. Weber, S. Motavalli, B. Fallahi, and S. H. Cheraghi, "A Unified Approach to Form Error Evaluation," *Precision Engineering,* vol. 26, no. 3, pp. 269-278, 2002.

[24] A. Malyscheff, T. Trafalis, and S. Raman, "From Support Vector Machine Learning to the Determination of the Minimum Enclosing Zone," *Computers & Industrial Engineering,* vol. 42, no. 1, pp. 59-74, 2002.

[25] C. Prakasvudhisarn, T. B. Trafalis, and S. Raman, "Support Vector Regression for Determination of Minimum Zone," *Journal of Manufacturing Science and Engineering,* vol. 125, no. 4, pp. 736-739, 2003.

[26] Y. Jiang, "Research on Many Measurement Points Flatness Error Intelligent Evaluation and Uncertainty Analytical Method," PhD Thesis, South China University of Technology, 2012.

[27] C. B. Barber, D. P. Dobkin, and H. Huhdanpaa, "The Quickhull Algorithm for Convex Hulls," *ACM Transactions on Mathematical Software (TOMS),* vol. 22, no. 4, pp. 469-483, 1996.

[28] G. Deng, G. Wang, and J. Duan, "A New Algorithm for Evaluating Form Error: The Valid Characteristic Point Method with the Rapidly Contracted Constraint Zone," *Journal of Materials Processing Technology,* vol. 139, no. 1-3, pp. 247-252, 2003.